ACS Catalysis

pubs.acs.org/acscatalysis
Research Article

Redox Properties of Pyrroloquinoline Quinone in Pyranose Dehydrogenase Measured by Direct Electron Transfer

Kota Takeda, James A. Birrell, Ryo Kusuoka, Tatsuki Minami, Kiyohiko Igarashi, and Nobuhumi Nakamura*

Cite This: ACS Catal. 2024, 14, 12242−12250
Read Online

ACCESS | Metrics & More | Article Recommendations | Supporting Information

ABSTRACT: Redox proteins regulate the chemical properties of cofactors through the protein environment of the active site. The redox potentials and pK_a values of the cofactors within the protein are crucial factors in determining the mechanism as they control the electron and proton transfer rates, respectively. The laborious determination of potentials and pK_a values using spectroscopic techniques can be avoided using direct electrochemistry. The aim of this work was to determine the redox potentials and pK_a values of pyrroloquinoline quinone (PQQ) in an enzyme with direct electron transfer (DET) using protein film voltammetry. While the redox properties of PQQ in aqueous and organic media have been studied, limited results of PQQ in an enzyme active site are available. Analysis of PQQ-dependent enzymes with direct electron transfer (DET) has been particularly difficult to establish. Here, we successfully observed redox waves of PQQ bound to the PQQ domain from the fungal PQQ-dependent pyranose dehydrogenase with a gold nanoparticle-modified electrode and determined the redox potentials at various pH values. Electron paramagnetic resonance (EPR) spectroscopy showed the formation of a PQQ semiquinone radical at an applied potential between the potentials of PQQ_{ox}/PQQ_{sem} and PQQ_{sem}/PQQ_{red}. These results clearly show that two-step one-electron transfer takes place via a semiquinone intermediate in the DET reaction. Both potentials shifted depending on pH; however, deviations from the $1e^-/1H^+$ behavior were observed at high pH. The pK_a of $PQQH^-/PQQH_2$ was determined to be close to neutral compared with a much higher value for free PQQ. At the physiological pH of this enzyme, which is neutral to slightly alkaline, the fully reduced form of PQQ was deprotonated, and both one-electron processes are very close in potential. This ensures a smooth energy landscape for optimal catalysis. Overall, these results show that the protein environment carefully tunes the properties of the PQQ cofactor for efficient catalysis involving both two-electron and one-electron chemistry.

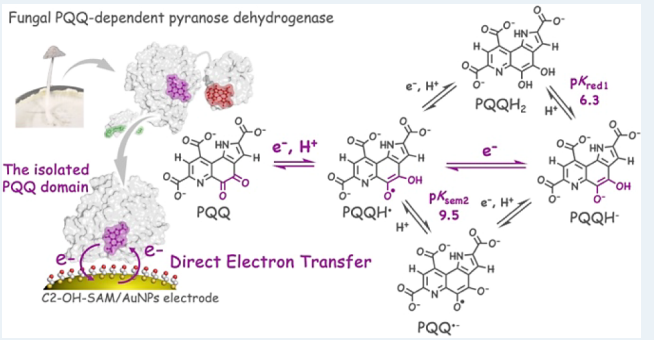

KEYWORDS: *direct electron transfer, pyrroloquinoline quinone, semiquinone radical, gold nanoparticles, dehydrogenase, EPR*

1. INTRODUCTION

Pyrroloquinoline quinone (PQQ) is an important redox cofactor alongside nicotinamide pyridine nucleotides (NAD(P)) and flavins (FAD, FMN). NAD(P) binds and dissociates with the NAD(P)-dependent enzymes, catalyzing the transfer of hydride ions (two electrons and one proton). FAD, FMN, and PQQ, on the other hand, are strongly bound to the enzyme and are reoxidized from reduced to oxidized forms within the enzyme in the catalytic cycle. Flavins and quinones can undergo not only one-step two-electron transfers (including hydride ion transfer) but also two-step one-electron transfers via radical intermediates. Thus, in charge transfer processes, they can mediate a hydride ion transfer reaction from NAD(P)H or an organic compound and a one-electron transfer reaction to a metalloprotein such as cytochrome.[1] PQQ is a two-electron carrier, and the redox reaction converts the orthoquinone moiety into the quinol. The reoxidation of fully reduced PQQ (PQQ_{red}) to fully oxidized PQQ (PQQ_{ox}) by cytochrome as a physiological one-electron acceptor proceeds in two one-electron steps via the PQQ semiquinone radical (PQQ_{sem}). The electron transfer behavior of PQQ can be described as follows in eqs 1 and 2 (proton transfer is not described here):

$$PQQ_{ox} + e^- \leftrightarrow PQQ_{sem} \quad (1)$$

$$PQQ_{sem} + e^- \leftrightarrow PQQ_{red} \quad (2)$$

where the PQQ_{sem} becomes a comparatively stable intermediate species in the enzyme. This is reflected by the redox

Received: April 19, 2024
Revised: July 17, 2024
Accepted: July 18, 2024
Published: August 1, 2024

potential of PQQ_{ox}/PQQ_{sem} (E_1) being slightly higher than that of PQQ_{sem}/PQQ_{red} (E_2). In contrast, free PQQ in buffered aqueous media commonly shows instability of the semiquinone radical (E_1 and E_2 are crossed). Therefore, only one voltammetric peak is typically observed, which can be considered to be a one-step, two-electron transfer.[2] This involves up to two proton transfers, dependent on the solution pH relative to the pK_a of the quinone moiety.[3,4] PQQ has several pK_a values attributable to single- and double-protonation of the oxidized, semireduced, and fully reduced states.[5] These values reflect protonation of the hydroxyl anion formed upon reduction of the quinone moiety. However, the pK_a values may be tuned by interaction of the protein surrounding with the pyridine, pyrrole, and three carboxylic acid functional groups of the PQQ molecule.[3−5] Furthermore, the pK_a values vary by metal ion coordination and protein−ligand interactions in the active site of the enzyme.[2] This in turn has made the proton-coupled electron transfer (PCET) reaction of enzyme-bound PQQ more complicated and interesting. The pH-dependent redox potential and pK_a values of PQQ have been well studied in aqueous and nonaqueous solutions.[4−7] In contrast, understanding PCET of PQQ in the active site of an enzyme is significantly more challenging, and very few studies have been conducted.[2,6] A relatively simple and straightforward method for investigating the redox states (potentials, pK_a, etc.) of cofactors in the protein environment is required.

PQQ-dependent enzymes were previously limited to bacteria, but recently, eukaryotic PQQ-dependent dehydrogenases were discovered in fungi.[9,10] Many genes encoding homologous enzymes are widely distributed in bacteria, archaea, amoebozoa, and fungi. Although the use of PQQ as a cofactor in mammalian enzymes remains unclear, it shows nutritional importance and pharmacological effects in mammals, including humans.[11] The question of why organisms use not only FAD but also PQQ as coenzymes is greatly interesting. PQQ features, for example, a redox potential that is roughly +0.25 V higher than that of FAD.[12] PQQ-dependent enzymes have a propeller superbarrel fold, large substrate pockets, and broad substrate selectivity. Metal ions such as Ca^{2+} bind PQQ, which is essential for catalytic activity. PQQ is bound mainly through hydrogen bonds to the active site and is not covalently linked.[13] It is unique in that exogenous PQQ can easily be incorporated into the apo-form of PQQ-dependent enzyme.[14]

Here, the pyranose dehydrogenase from the basidiomycete *Coprinopsis cinerea* (*Cc*PDH) has been used.[9,15] It would secrete the extracellular environment as apo-form and utilizes exogenous PQQ. The enzyme is thought to be related to the enzymatic degradation of plant cell walls by donating an electron to copper-containing monooxygenases via its own cytochrome domain. Although the physiological substrate is still controversial, this enzyme catalyzes the oxidative dehydrogenation of various aldose sugars.[16] The full-length *Cc*PDH consists of the catalytic PQQ domain, an N-terminal cytochrome *b* domain, and a C-terminal cellulose-binding domain (Figure 1a). The oxidation of the substrate takes place in the catalytic domain, followed by interdomain electron transfer (IET) from the reduced PQQ cofactor to the heme *b* in the cytochrome domain. It has been suggested that the IET is dependent on pH and is a rate-limiting step in the pH range from 6.0 to 8.5[17,18] In this study, the cytochrome domain of *Cc*PDH, the electron acceptor from PQQ, was replaced by an

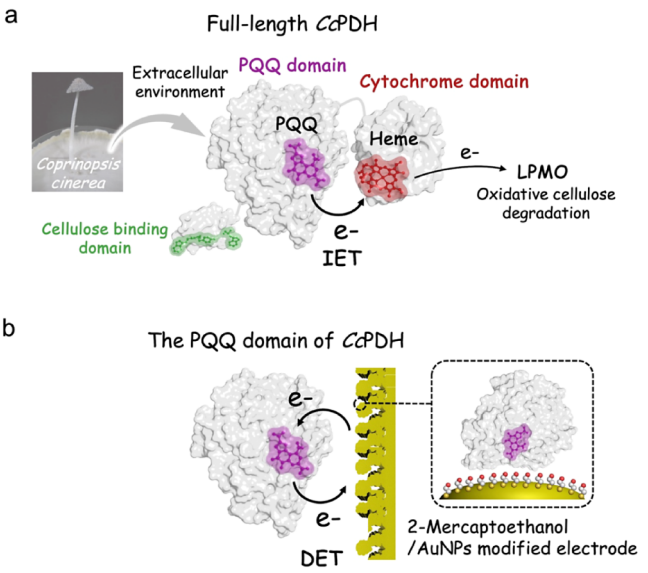

Figure 1. (a) Schematic representation of full-length *Cc*PDH and the electron transfer pathways. Pyranose oxidation takes place at the PQQ domain, followed by IET to the cytochrome domain. Subsequent to the reduction of the heme, the electron is delivered to lytic polysaccharide monooxygenase (LPMO). (b) Schematic of DET of the PQQ domain of *Cc*PDH on ME/AuNPs/AuE.

electrode, and the redox potentials and electron transfer of PQQ in the enzyme were investigated by analyzing the direct electron transfer (DET) of the isolated PQQ domain (Figure 1b).

Protein film voltammetry provides a powerful way to investigate the mechanisms of electron transfer processes and chemical reactions coupled to them that occur at the active sites of proteins.[19−21] DET occurs when electrons are transferred between an electrode and a redox protein in contact without any electron mediators. Current−potential curves obtained from DET-type reactions deliver various kinds of information on the redox enzymes and can be used as a tool for mechanistic studies.[22] Enzymatic biosensors and biofuel cells based on DET have also attracted attention.[22−24] DET-type enzymes such as hydrogenases, multicopper oxidases, fructose dehydrogenase, and cellobiose dehydrogenase are mostly multicofactor-containing enzymes that have redox sites that play a role in electron transfer (i.e., heme, Fe−S cluster, type I copper) in addition to a catalytic site.[25−27] PQQ-dependent dehydrogenases are commonly studied as bioelectrocatalysts for bioelectronic devices.[28] Membrane-bound PQQ-dependent alcohol dehydrogenase was the first reported DET-type bioelectrocatalytic PQQ enzyme. The enzyme has an additional prosthetic group, a heme, which acts as a built-in electron mediator from PQQ to the electrode.[29]

The catalytic centers of enzymes are usually buried within the protein structure and are covered by an electrically insulating protein shell. Although it is often difficult to obtain DET from the catalytic center, several studies of DET have been reported for single-cofactor enzymes with only one active center (e.g., horseradish peroxidase,[30] ferredoxin-$NADP^+$ reductase,[31] the PQQ domain of pyranose dehydrogenase,[32,33] and FAD-dependent glucose dehydrogenase[34]). DET strongly depends on the 3D structure of the enzyme. Due to this problem, it has been attempted to make DET more efficient by fabricating nanostructured electrodes, by designing methods

https://doi.org/10.1021/acscatal.4c02319
ACS Catal. 2024, 14, 12242−12250

for immobilizing these enzymes on electrodes, or by protein engineering of enzymes. Among single-cofactor type PQQ-dependent enzymes, a few studies reported on DET of soluble PQQ-dependent glucose dehydrogenases (sGDH) with nanomaterial-modified electrodes. However, catalytic currents for glucose oxidation were observed in this work with a higher potential than the redox potential of PQQ.[35−37] In addition, there was some variability in the reported number of PQQ redox peaks as well as in the potential values for enzymes measured with cyclic voltammetry under nonturnover conditions (in the absence of enzymatic substrate). Flexer et al. reported that two redox peaks in the anodic scan, at −159 and +145 mV (vs AglAgCl reference electrode, pH 7.2), were observed for sGDH immobilized on a carbon cryogel electrode.[37] The peak potentials of both, particularly the latter, appear to be shifted in a positive direction compared with the original redox potential of PQQ in the enzyme. The authors suggested that this could be due to slow and irreversible electron transfer on the electrode surface. The direct electrochemistry of PQQ in enzymes is not yet fully understood.

The current paper demonstrates a DET reaction of a single-cofactor type PQQ-dependent enzyme and studies the redox potentials and pK_a values of its PQQ cofactor. The enzyme used in the present work is the PQQ domain (containing only the PQQ cofactor), which is separated from the full-length *Cc*PDH. Previous work already showed that the PQQ domain was able to engage in DET-type bioelectrocatalysis without its built-in mediator cytochrome domain.[32] In the present work, we have undertaken electrochemical analyses together with spectroscopic studies on PQQ in the active site of *Cc*PDH. In cyclic voltammograms (CVs) of DET with a catalytic reaction, signals (i.e., catalytic current) are amplified by bioelectrocatalysis and, thus, are easier to observe than the noncatalytic signal in the absence of substrate. On the other hand, in CVs of DET without the catalytic reaction, noncatalytic current signals resulting from the redox reaction of enzymes are often difficult to monitor due to the fact that they are buried in nonfaradaic currents. The reason is that the current intensity depends on the amount of electroactive enzyme on the electrode surface. To obtain distinct signals from redox centers in the protein requires various techniques to improve adsorption, orientation, and electron transfer rate, e.g., a 3D-structured and chemically modified electrode surface. Fabrication of gold nanoparticles (AuNPs) can produce 3D-surface structured electrodes that yield a large surface area-to-volume ratio and thus can increase protein loading. Furthermore, a self-assembled monolayer composed of 2-mercaptoethanol is known to give excellent DET-type bioelectrocatalysis for the PQQ domain.[32] Hence, we investigated the direct redox reaction of the PQQ domain with AuNPs and a coated 2-mercaptoethanol SAM-modified electrode (Figure 1b). In this study, the redox potential of PQQ in the active site of the enzyme was measured by the DET, and its pH dependence was used to analyze the pK_a values and redox potentials.

2. MATERIALS AND METHODS

2.1. Materials. The isolated dehydrogenase domain (PQQ domain: residues 240−649, 45 kDa) from *Cc*PDH was obtained according to our previous report.[9] Briefly, the recombinant PQQ domain was produced in *Pichia pastoris* and purified from the culture filtrate using ammonium sulfate fractionation and two-step column chromatography (TOYOPEARL phenyl-650S column, Tosoh Corp.; UNO S6 column, Bio-Rad Laboratories, Inc.). Deglycosylation of the recombinant enzyme was performed using endo-*β*-*N*-acetylglucosaminidase H. Reconstitution of the apoenzyme was carried out with a 10-fold molar excess of PQQ in 20 mM acetate buffer, pH 6.0, containing 1 mM $CaCl_2$ at 4 °C for 3 h. The free PQQ was completely removed by buffer exchange with Vivaspin 20−5K (GE Healthcare). The PQQ domain concentration was determined by using the molar absorption coefficient of 72 410 M^{-1} cm^{-1} at 280 nm. 2-Mercaptoethanol was purchased from Tokyo Chemical Industry Co., Ltd. (Tokyo, Japan). L-Fucose was purchased from Sigma-Aldrich Japan G. K. (Tokyo, Japan). Pyrroloquinoline quinone disodium salt, trisodium citrate dehydrate, and hydrogen tetrachloroaurate (III) tetrahydrate (H_4AuCl_4) were purchased from FUJIFILM Wako Pure Chemical Corp. (Osaka, Japan).

2.2. Electrochemical Experiments. Following our previously reported procedure, an AuNPs-modified gold electrode was prepared as a working electrode.[32,38] AuNPs with a particle diameter of 14−15 nm were prepared by citric reduction of H_4AuCl_4 with reference to Frens.[39] The obtained AuNPs solution was centrifuged (10 000 g, 30 min), and then the precipitated AuNPs were suspended by ultrasonication as a 50-fold concentrated AuNPs dispersion. 1 *μ*L portion of the concentrated AuNPs was added onto the surface of a polycrystalline gold electrode (diameter 1.6 mm, AuE) and then air-dried. The drop-casted AuNPs electrodes (AuNPs/AuEs) were obtained by repeating this process three times. AuNPs/AuEs were cleaned in 0.5 M H_2SO_4 by cyclic voltammetry between −0.2 and +1.5 V vs AglAgCl (3 M NaCl) for 20 cycles at a scan rate of 0.1 V s^{-1} before modifying with a self-assembled monolayer (SAM). SAM-modified AuNPs/AuEs were prepared by immersion in 20 mM 2-mercaptoethanol (in H_2O) for 1 h at room temperature. The SAM-modified electrode (ME/AuNPs/AuE) surface was rinsed with Milli-Q water to remove the excess thiol molecules. The PQQ domain was adsorbed on ME/AuNPs/AuEs using 10 *μ*L of 1 *μ*M holo-PQQ domain in a 20 mM sodium acetate buffer solution, pH 6.0 at 4 °C for over 10 h. Before each measurement, the electrodes were gently rinsed with the same buffer to remove the weakly adsorbed enzyme. CV was conducted using an ALS Model 612Dx electrochemical analyzer (BAS Inc., Tokyo, Japan). A conventional three-electrode cell was used in which a platinum wire served as the counter electrode and AglAgCl (3 M NaCl) served as the reference electrode. Before the measurements, N_2 bubbling was used to remove oxygen from the solutions in the electrochemical cell. All the potentials cited in this paper are with respect to the AglAgCl (3 M NaCl) electrode, with a potential of +209 mV vs the normal hydrogen electrode (NHE). CV measurements were performed in 50 mM acetate buffer, pH 6.0, at ambient temperature. The following buffers were used for studies of the pH dependence: 50 mM sodium acetate from pH 4.6 to 6.0, 50 mM MES at pH 6.6, 50 mM HEPES from pH 7.0 to 7.6, 50 mM Tris−HCl from pH 8.0 to 9.5, and 50 mM CAPS at pH 9.9.

2.3. EPR Experiments. Electron paramagnetic resonance (EPR) samples of 200 *μ*M holo-PQQ domain in 50 mM acetate buffer pH 6.0, were prepared in an anaerobic glovebox and poised at various potentials using a redox mediator cocktail (1 *μ*M each of 2,6-dichlorophenolindophenol, potassium 5,5′,7,7′-indigotetrasulfonate, methylene blue, 1,2-naphthoquinone, and phenazine methosulfate). The solution potential was

https://doi.org/10.1021/acscatal.4c02319
ACS Catal. 2024, 14, 12242−12250

measured using a home-built two-electrode electrochemical cell with a glassy carbon working electrode and a KCl-saturated AgAgCl counter/reference electrode and adjusted by the addition of small amounts of sodium dithionite or potassium ferricyanide. Once the potential was stable, samples were transferred to 0.4 mm diameter quartz EPR tubes and frozen in liquid nitrogen. Samples were measured on a MiniScope MS 5000 benchtop X-band (9.5 GHz) EPR spectrometer (Magnettech) by using a nitrogen gas cooling stream to set the temperature to 150 K. EPR spectra were recorded with a 10 μW microwave power. Data were processed using home-written routines.

3. RESULTS AND DISCUSSION

3.1. Cyclic Voltammetry. Nanostructured electrodes were prepared by drop-casting citrate-reduced AuNPs three times on the surface. The 2-mercaptoethanol SAM is responsible for the physical adsorption of the enzyme (mainly by hydrogen bonding) and for aligning its orientation to the electrode interface. The AuNPs-modified electrode allows the observation of well-defined surface redox waves under conditions where no catalysis is occurring, which are invisible on the flat gold electrode. We considered the redox reaction of the PQQ domain when the nonturnover redox reaction was analyzed without substrate at pH 6.0, since pH 6.0 is optimal for the catalytic activity.

As shown in Figure 2a,b, two pairs of coupled cathodic and anodic peaks were observed. The linear dependence of peak currents on the scan rate was in accord with those expected for surface-immobilized electrochemical behavior (Figure 2c,d). Since two redox peaks were observed, the electron transfer between PQQ and the electrode can be considered as two one-electron transfer steps via a semiquinone radical state. The peak widths at half height of oxidation and reduction of E_1 were 97 and 87 mV, and that of E_2 were 104 and 86 mV, respectively (calculated from Figure 2b), indicating that these agree with 1e$^-$ processes (ideally 90 mV under these conditions). These peaks of E_1 and E_2 are the result of the redox reaction of the PQQ cofactor inside the enzyme and correspond to the redox potential of eqs 1 and 2, respectively. The midpoint potentials of E_1 and E_2 were -63 ± 4 mV and -208 ± 2 mV, respectively (vs AgAgCl, 3 M NaCl, at pH 6.0). Electroactive coverage of the enzyme on the electrode (Γ_E) was estimated by integrating the observed nonturnover CV curve oxidation peak in Figure 2a using the following equation: $\Gamma_E = Q/nFA$. Q is the charge involved in the reaction, and n is the number of electrons involved in the redox process (for E_2 oxidation, $n = 1$), resulting in an estimate of Γ_E of 34 ± 2 pmol cm^{-2} (with reference to the geometrical surface area (A, 0.0201 cm^2)). Using the amount of enzyme on the obtained electrode, the value of the catalytic constant (k_{cat}) for the PQQ domain of *Cc*PDH in bioelectrocatalysis for L-fucose oxidation of a similarly prepared enzyme-immobilized ME/AuNPs/AuE was determined (Figure S1). This value, 56.7 s^{-1}, was in close agreement with the k_{cat} value in the solution assay,[17] approximately 50 s^{-1}. The results indicate that the enzyme maintains its natural conformation and activity when it is bound to the electrode.

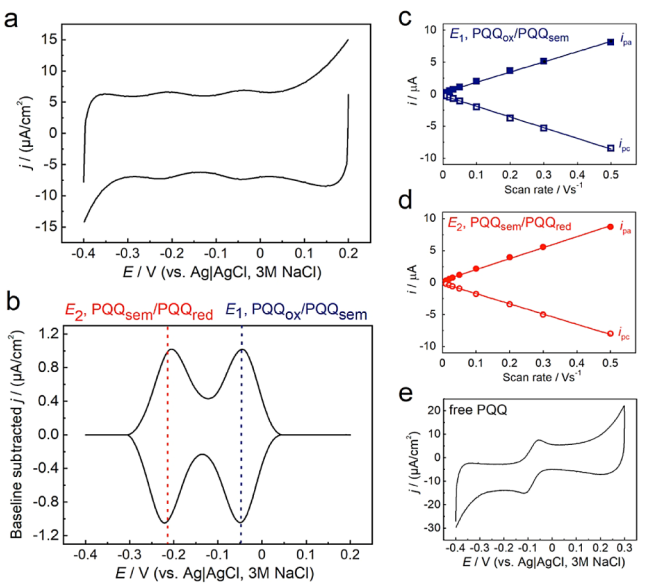

Figure 2. CVs of the PQQ domain of *Cc*PDH on ME/AuNPs/AuE in 50 mM sodium acetate, pH 6.0, at 25 °C under nonturnover conditions (absence of substrate): (a) raw data; (b) baseline-subtracted data. The data were used to obtain peak potentials. Scan rate = 10 mV s^{-1}. Plots of anodic (i_{pa}) and cathodic peak current (i_{ca}) versus scan rate for (c) redox reaction of PQQ_{ox}/PQQ_{sem}, and (d) PQQ_{sem}/PQQ_{red} on the PQQ domain on ME/AuNPs/AuE in 50 mM acetate buffer, pH 6.0, at 25 °C. (e) CV of 100 μM PQQ with ME/AuNPs/AuE in 50 mM acetate buffer, pH 6.0, at 25 °C. Scan rate = 10 mV s^{-1}.

The electroactive surface area of the AuNPs-modified electrode was estimated from the voltammogram by integrating the gold oxide reduction peak. The electroactive surface area of the 3-times drop-casted AuNPs electrode (in this case) increased 56-fold compared to a flat-polycrystalline gold electrode.[32] The value of 34 pmol cm^{-2} (with reference to the geometrical surface area) corresponds to an adsorption density per electroactive surface area of approximately 0.6 pmol cm^{-2}. The theoretical maximum number of PQQ domain molecules that can be adsorbed onto a surface is calculated to be 7.6 pmol of cm^{-2}. Thus, the PQQ domain can be adsorbed on approximately 10% of the electroactive surface area of the AuNPs electrodes. This may be due to the large number of meso- and microspaces below the size of the enzyme molecule on the AuNPs electrodes, which means that there are numerous sites where the enzyme cannot be adsorbed.

Kanninen et al. reported that the PQQ compound (not in an enzyme) immobilized on glassy-carbon electrodes modified with single-walled carbon nanotubes shows a redox potential of -90 mV (vs AgAgCl, 3 M KCl, at pH 6.0), which is a single reversible two-electron transfer redox process.[7] The CV was run with ME/AuNPs/AuE that was unmodified with the enzyme in the same buffer (50 mM sodium acetate, pH 6.0) containing 0.1 mM free PQQ (Figure 2e). A single reversible redox process was observed with an apparent half-wave potential equal to -85 mV vs AgAgCl, 3 M NaCl. The redox potential of free PQQ in an aqueous solution was different from both the two redox potentials of the PQQ domain and slightly more positive than the average of E_1 and E_2 (-136 mV). The dramatic change from one 2e$^-$ step to two 1e$^-$ steps and the more negative average redox potential likely reflect the interaction of PQQ with Ca^{2+} and amino acids in the protein environment that tune the PQQ properties. The interactions in the protein environment that influence the potential must be investigated in detail. For example, reduced forms of flavins and quinones are destabilized by hydrophobic

https://doi.org/10.1021/acscatal.4c02319
ACS Catal. 2024, 14, 12242−12250

environments, decreasing the cofactor redox potential but also favoring coupled protonation to compensate for the large amount of negative charge.[40−42] On the other hand, hydrogen bonding and metal-ion coordination stabilize the reduced forms, shifting the redox potential in a positive direction, disfavoring protonation.[40] The balance of these interactions and the solvents etc. will affect the redox potential of the cofactors in the proteins. In this work, hydrophobic interactions within the active site of the *Cc*PDH appeared to dominate, lowering the average potential of PQQ compared to that of free PQQ in buffer aqueous solution. This is relatively favorable for the transfer of electrons to the physiological electron acceptor heme because the driving force for electron transfer is greater.

Here, we wish to emphasize that the electrochemistry for the PQQ domain immobilized electrodes, including in previous works,[32,33] results from the direct redox reaction of the PQQ cofactor buried inside the enzyme, not the redox reaction of electron mediated by free PQQ (e.g., by loss of PQQ from the enzyme). Two pairs of redox peaks associated with two one-electron steps were observed in the CV for the enzyme electrode, while one pair of redox peaks with one two-electron step was shown in the CV of free PQQ (Figure 2). Under turnover conditions, initially PQQ is reduced by two electrons from L-fucose as substrate in the reductive half-reaction. Following product release, the complete oxidation half-reaction (i.e., reoxidation of $PQQH_2$ to PQQ) occurs before a second L-fucose can be oxidized. Therefore, ideally, the oxidative catalytic current will titrate with the redox potential of PQQ_{ox}/PQQ_{sem} provided electron transfer is not rate-limiting. Previous results show that the center of the catalytic wave (i.e., the half-wave potential at which the current is equal to half of the catalytic current) starts around −50 mV (Figure 5 in ref 32), which corresponds to the redox potential of PQQ_{ox}/PQQ_{sem}, E_1, and is more positive than that of free PQQ.

3.2. EPR Signals Response to Potential. The semiquinone form of PQQ can be studied by EPR spectroscopy. PQQ semiquinone radical formation was confirmed by the detection of an isotropic EPR signal around g = 2.0065 in samples of the PQQ domain poised at a potential of −125 mV (close to the average of the two midpoint potentials E_1 and E_2) (Figure 3). This X-band cw-EPR signal is similar to that observed in sGDH[2] and *Pseudomonas aeruginosa* ethanol dehydrogenase (QEDH).[8] The EPR signal was much smaller at potentials of −325 and +90 mV, below and above the values of E_1 and E_2, respectively. The results suggested that the PQQ semiquinone radical in the PQQ domain is generated on the electrode at applied potentials between E_1 and E_2.

3.3. pH-Dependent Redox Potential and pK_a Values. We next measured cyclic voltammetry of the PQQ domain of *Cc*PDH at pH values from 4.5 to 10.0 (Figure S1). At low pH, two clearly reversible one-electron waves are observed. As the pH increases, both peaks move toward more negative potential, indicating proton-coupled electron transfer is occurring for both redox transitions. Above pH 6.0, the E_2 potential starts to become pH-independent and the separation between E_1 and E_2 starts to diminish. Around pH 8.0, the E_1 and E_2 peaks overlap, suggesting that their potentials are very close, possibly crossing over. Analysis of the CVs was performed using a two-electron model in QSoas software,[43] in which an average E value and ΔE value ($E_2 - E_1$) are extracted. This analysis allowed the potentials to be extracted for all of the pH values, including the overlap region of the peaks. The average E_1 and E_2 potentials are plotted vs pH in Figure 4 and are fitted with a simple two-electron two-proton model reported by Hirst.[44] Excellent fits were achieved with E_{alk1} ($PQQ/PQQ^{\bullet-}$) = −266 mV and E_{alk2} ($PQQ^{\bullet-}/PQQ^{2-}$) = −281 mV with pK_{ox1} ($PQQH^+/PQQH_2^{2+}$) < 4.0, pK_{ox2} ($PQQ/PQQH^+$) < 5.0, pK_{sem1} ($PQQH^{\bullet}/PQQH_2^{\bullet+}$) < 4.0, p$K_{sem2}$ ($PQQH^{\bullet}/PQQ^{\bullet-}$) = 9.5, p$K_{red1}$ ($PQQH^-/PQQH_2$) = 6.3, and pK_{red2} ($PQQH^-/PQQ^{2-}$) = 10.3. More precise values of pK_{ox1}, pK_{ox2}, and pK_{sem1} could not be obtained due to the fact that the protein was unstable below pH 4.5. Regardless, the fits were quite sensitive to the other pK_a values and the E values, and so we can be confident about their accuracy. To summarize these results, a thermochemical square scheme of PQQ with pK_a values and redox potentials is presented in Figure 5. The results indicate that the PQQ radical is protonated at neutral to low pH and that the fully reduced PQQ is doubly protonated only at very low pH but do not clarify whether reduced PQQ is deprotonated at which O-5 or O-4 first. In the bacterial quinoprotein ethanol dehydrogenase, ENDOR and DFT calculations suggested that reduced PQQ of is unlikely to be protonated at O-5, at pH 8.0, by Kay et al.[8] Thus, we depicted the first deprotonation from O-5. The results confirm that the redox reaction of PQQ_{ox}/PQQ_{sem} is a

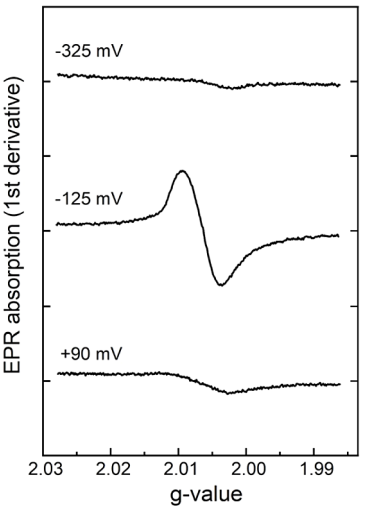

Figure 3. X-band (9.5 GHz) CW EPR spectra of the PQQ domain under equilibrium solution potentials of −325, −125, and +90 mV vs Ag|AgCl 3 M KCl.

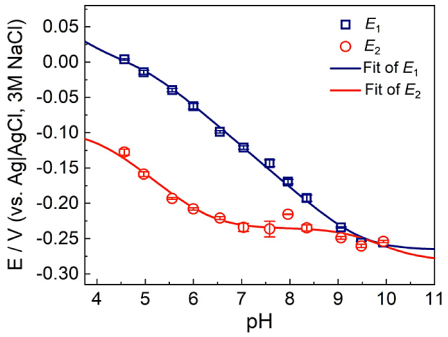

Figure 4. Plots of the redox potentials against pH for E_1 (PQQ_{ox}/PQQ_{sem}, square) and E_2 (PQQ_{sem}/PQQ_{red}, circle) in the PQQ domain. Fitting of the plots to the Nernst equation with acid dissociation equation for E_1 (navy blue) and E_2 (red).

https://doi.org/10.1021/acscatal.4c02319
ACS Catal. 2024, 14, 12242−12250

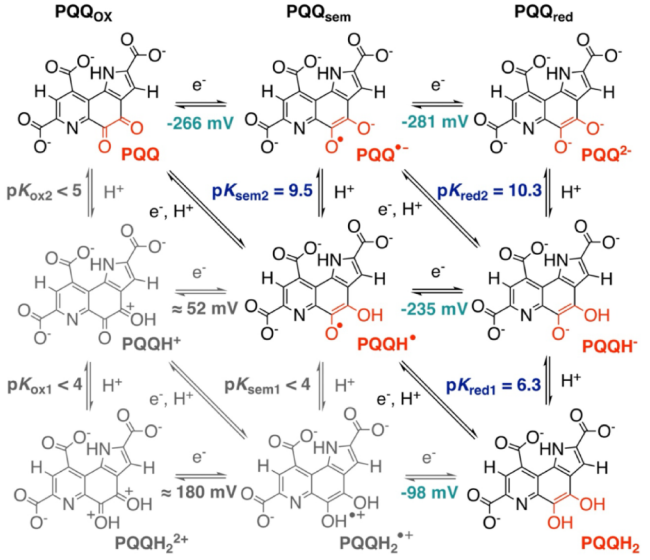

Figure 5. Schematic of PQQ electron, proton, and proton-coupled electron transfer in the enzyme with obtained values of pK_a and redox potential.

1e$^-$/1H$^+$ transfer over the pH range 4.0−9.0, while PQQ$_{sem}$/PQQ$_{red}$ is a 1e$^-$/1H$^+$ transfer in the acidic region but a 1e$^-$ transfer in the pH range 6.5−9.0. Hence, E_1 decreases from the acidic side to pH 9.0, whereas E_2 does not decrease from around neutral. The potential difference between E_1 and E_2 is reduced at pH > 6.0. At higher pH, the two one-electron waves merged into a single two-electron wave.

The pK_{red1} of 6.3 was determined in the enzyme-bound PQQ, which is lower than Kano et al. reported the pK_{a1}, (PQQH$^-$/PQQH$_2$) of the free PQQ compound in aqueous media, being at 8.5.[5] The calcium ion ligand at the active site probably contributes to the decrease in the pK_{red1}. In the PQQ domain, Ca^{2+} is a seven-coordinate pentagonal bipyramid with ligands from O-5, N-6, and carboxylate −7' of PQQ, the side chain carboxylate of Asp451, a carbonyl oxygen atom of Ser449 in the main chain, and two water molecules.[45] Generally, Lewis acidic metal ions decrease the pK_a of ligands because the formation of coordination bonds promotes the polarization of O−H bonds and neutralizes and stabilizes the negative charge of the alkoxide ion generated by deprotonation. For example, the pK_a (QH$^-$/QH$_2$) is 2 units smaller for Ca^{2+}-complexed calix[4]arene-triacid-monoquinone (CTAQ), a quinone-containing water-soluble ionophore as a model compound, than for free CTAQ.[46]

3.4. Stability of the Semiquinone Intermediate. The thermodynamic stability of the semiquinone is reflected in the difference between E_{ox}/E_{sem} and E_{sem}/E_{red}. The semiquinone formation constant (K_{sem}) is given by[2]

$$K_{sem} = \exp[F/RT(E_1 - E_2)]$$

The midpoint potentials of the PQQ domain at pH 7.0 were $E_1 = -121 \pm 2.5$ mV and $E_2 = -234 \pm 5.8$ mV in our case. The value was calculated to be $K_{sem} = 81$. Sato et al. reported that the spectroelectrochemically determined redox potentials of PQQ for sGDH in buffered solution were $E_{ox/sem} = -176$ mV and $E_{sem/red} = -221$ mV ($K_{sem} = 5.7$) at pH 7.0 (describing converted values vs Ag|AgCl 3 M NaCl).[2] Although there may be some differences in the measurement method for the redox potentials, the results suggest that the semiquinone radical is more stabilized in *Cc*PDH than in sGDH. As a consideration, the indole−nitrogen atom of Trp563 is located 3.5 Å above the pyridine ring of PQQ in the PQQ domain of *Cc*PDH. It is possible that the lone-pair (N atom of Trp)−π (PQQ) interaction contributes to the delocalization of spin density and stabilizes the semiquinone radical (Figure S3). On the other hand, Tyr343 in sGDH, which corresponds to Trp563 in *Cc*PDH, is 4.4 Å away from the pyridine ring of PQQ, a bit far to make the lone-pair−π interaction.

3.5. Electron Transfer Rates. In Figure 6, anode and cathode peak potentials for E_1 and E_2 are plotted versus the

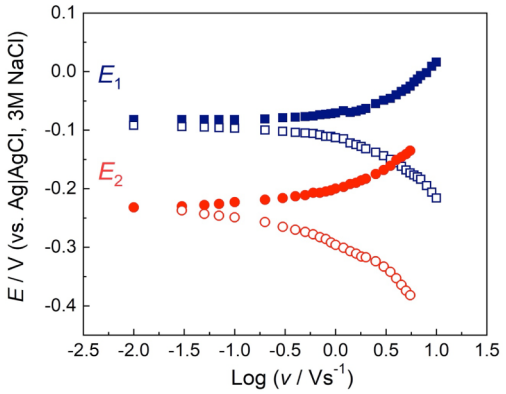

Figure 6. Laviron plot of the PQQ domain of *Cc*PDH on ME/AuNPs/AuE in 50 mM sodium acetate, pH 6.0, presenting the evolution of the anodic (filled) and cathodic (open) peak potentials of E_1 (square) and E_2 (circle) as a function of the natural logarithm of the scan rate.

logarithm of the scan rate (scan rate, v, over the range 0.01−10 V s^{-1}, at pH 6.0). The symmetrical peak separation increased with an increasing scan rate, resulting in a typical trumpet plot. Accordingly, the values of the standard rate constants (k_{ET}) were determined using the Laviron method.[47] The analysis gives the k_{ET} values and transfer coefficient (α) values shown in Table 1. The k_{ET} for the redox reaction of PQQ$_{sem}$/PQQ$_{red}$ was about half as slow as that of PQQ$_{ox}$/PQQ$_{sem}$. The pK_a-value for the reduced species (pK_{red1} = 6.3) is lower than that for the semiquinone species (pK_{sem2} = 9.5) and close to the pH of the solvent (pH 6.0). The reaction of PQQ$_{ox}$/PQQ$_{sem}$ occurs by proton-coupled electron transfer, whereas simple electron transfer would be dominant in the PQQ$_{sem}$/PQQ$_{red}$ reaction. This difference may affect the kinetics. Both of the k_{ET} values for reduction slowed down to half of that for the oxidation.

Table 1. Electron Transfer Rates between PQQ in the Enzyme and Electrodes in the Redox Reactions of PQQ$_{ox}$/PQQ$_{sem}$ and PQQ$_{sem}$/PQQ$_{red}$

		α	k_{ET} (s^{-1})
PQQ$_{ox}$/PQQ$_{sem}$	oxidation	0.5	32.7
	reduction	0.5	24.0
PQQ$_{sem}$/PQQ$_{red}$	oxidation	0.5	16.1
	reduction	0.5	8.6

Based on the above, we can discuss the catalytic reaction of *Cc*PDH. The two intrinsic one-electron redox potentials of the deprotonated PQQ are quite similar, but interaction with the protein surroundings tunes the pK_a values so that in a pH

https://doi.org/10.1021/acscatal.4c02319
ACS Catal. 2024, 14, 12242−12250

range (6.0−9.0), the first reduction is coupled to protonation, while the second reduction is not coupled to protonation. The $PQQH^-$ state is supported by the observations made for the PQQ-dependent ethanol dehydrogenase.[8] The fact that the reduced form is $PQQH^-$ eliminates a scheme in which the catalytic residue adds a proton drawn from the substrate to the PQQ (rearrangement) in the catalytic cycle. This would seem to be advantageous to the catalytic reaction. The pK_{red1} of 6.3 in the enzyme-bound PQQ was lower than that of free PQQ in aqueous media, being 8.5. This means that reduced PQQ is singly protonated ($PQQH^-$) in the pH range where the enzymatic activity of the PQQ domain is sufficiently large. Furthermore, the pK_{sem2} of PQQ in the enzyme was 9.5 compared to free PQQ of 8.7, favoring the $PQQH^\bullet$ state of semiquinone. Thus, the redox reaction of PQQ was suggested to be a two-electron and one-proton transfer during the physiological pH range. This may help the enzyme maintain efficient catalysis across the pH range where the enzymatic activity via the interdomain electron transfer of *Cc*PDH is maximized at higher pH.

4. CONCLUSIONS

Protein film voltammetry of fungal PQQ-dependent dehydrogenase immobilized on AuNPs-modified electrodes based on DET provides a unique opportunity to investigate the mechanism of PQQ PCET in the protein. The results of this research, e.g., potentials, rate constants, and surface concentration of the enzyme, are important in further understanding the DET-type bioelectrocatalysis. Furthermore, this study contributes to the fundamental understanding of enzymes containing PQQ cofactors including their reaction mechanism with PCET. It will also be useful to analyze the influence of interactions with amino acid residues around the active site and the binding of metal ions on the redox properties of the PQQ cofactor.

The results are consistent with those published previously and with the known values of potentials from spectroelectrochemical analysis. The observed redox waves in the present case are caused neither by a shift of the peak potentials from the original potentials of PQQ due to overvoltage, etc., as seen in the CV of sGDH, nor by leakage of PQQ from the protein. At low pH, CV showed two reversible pairs of redox waves, indicating two one-electron steps for the redox reaction of PQQ in the enzyme. EPR spectroscopy revealed the formation and disappearance of the PQQ semiquinone radical in the enzyme before and after each potential. These results provide evidence that the reaction involves two one-electron steps via a $PQQH^\bullet$ radical. The pK_a values were obtained from the analysis of an *E* versus pH plot with the Nernst equation and the acid dissociation equation. In PQQ bound to the enzyme, the potential was reduced (ΔE = −51 mV) and pK_{red1} was approximately 2 units smaller compared to free PQQ in buffered solution. As often seen in other cofactor-containing enzymes, the enzyme is shown to regulate the potential and pK_a of PQQ in the active site. This regulation appears to maintain the enzyme activity in the pH range of the physiological environment in which *Cc*PDH is presumed to be secreted extracellularly to work. Basically, our study provides further support for the idea that proteins have a substantial influence on the cofactors to which they bind. In the case of PQQ in *Cc*PDH, the average redox potential is tuned to be closer to the substrate or product potentials for minimizing energy loss or enhancing electron transfer rates, and the two one-electron potentials are split so that the PQQ can engage in efficient two-electron and one-electron chemistry required for substrate oxidation and subsequent electron transfer. How exactly the protein environment regulates catalysis and intra- or interprotein electron transfer is expected to be clarified in future studies. In the future, it will be interesting to probe the local environment using site-directed mutagenesis to learn which amino acids are crucial in influencing the redox properties of PQQ. This might allow PQQ-based enzymes to be tailored for specific applications.

■ ASSOCIATED CONTENT

Supporting Information

The Supporting Information is available free of charge at https://pubs.acs.org/doi/10.1021/acscatal.4c02319.

Enzymatic turnover rate of the PQQ domain of *Cc*PDH on the electrode; cyclic voltammograms of the PQQ domain of *Cc*PDH at various pH; and structure of the active site in the PQQ domain of *Cc*PDH (PDF)

■ AUTHOR INFORMATION

Corresponding Author

Nobuhumi Nakamura − *Department of Biotechnology and Life Science, Tokyo University of Agriculture and Technology, Koganei, Tokyo 184-8588, Japan;* orcid.org/0000-0002-5373-2972; Phone: +81-42-3887482; Email: nobu1@cc.tuat.ac.jp; Fax: +81-42-3887482

Authors

Kota Takeda − *National Institute of Advanced Industrial Science and Technology, Sendai 983-8551, Japan*

James A. Birrell − *School of Life Sciences, University of Essex, Colchester CO4 3SQ, U.K.;* orcid.org/0000-0002-0939-0573

Ryo Kusuoka − *Department of Biotechnology and Life Science, Tokyo University of Agriculture and Technology, Koganei, Tokyo 184-8588, Japan*

Tatsuki Minami − *Department of Biotechnology and Life Science, Tokyo University of Agriculture and Technology, Koganei, Tokyo 184-8588, Japan*

Kiyohiko Igarashi − *Department of Biomaterial Sciences, Graduate School of Agricultural and Life Sciences, The University of Tokyo, Tokyo 113-8657, Japan*

Complete contact information is available at: https://pubs.acs.org/10.1021/acscatal.4c02319

Notes

The authors declare no competing financial interest.

■ ACKNOWLEDGMENTS

The authors would like to thank Prof. Wolfgang Lubitz, Max Planck Institute for Chemical Energy Conversion, for the support with EPR measurement and writing the manuscript. Funding was provided by a Grant-in-Aid for Young Scientific Research (grant no. 22K14826 to K.T.). J.A.B. acknowledges funding from the DFG SPP 1927 "Iron−Sulfur for Life" project (Project No. BI 2198/1-1) and funding from the Max Planck Society.

■ REFERENCES

(1) Kano, K.; Shirai, O.; Kitazumi, Y.; Sakai, K.; Xia, H.-Q. *Enzymatic Bioelectrocatalysis*; Springer; 2021.

(2) Sato, A.; Takagi, K.; Kano, K.; Kato, N.; Duine, J. A.; Ikeda, T. Ca Stabilizes The Semiquinone Radical of Pyrroloquinoline Quinone. *Biochem. J.* **2001**, *357*, 893−898.
(3) Itoh, S.; Kawakami, H.; Fukuzumi, S. Electrochemical Behavior and Characterization of Semiquinone Radical Anion Species of Coenzyme PQQ in Aprotic Organic Media. *J. Am. Chem. Soc.* **1998**, *120* (29), 7271−7277.
(4) Kano, K.; Mori, K.; Uno, B.; Kubota, T.; Ikeda, T.; Senda, M. Voltammetric Determination of Acid Dissociation Constants of Pyrroloquinoline Quinone and Its Reduced Form under Acidic Conditions. *J. Electroanal. Chem. Interfacial Electrochem.* **1990**, *299* (2), 193−201.
(5) Kano, K.; Mori, K.; Uno, B.; Kubota, T.; Ikeda, T.; Senda, M. Voltammetric and Spectroscopic Studies of Pyrroloquinoline Quinone Coenzyme under Neutral and Basic Conditions. *Bioelectrochem. Bioenerg.* **1990**, *23* (3), 227−238.
(6) Nakamura, N.; Kohzuma, T.; Suzuki, S. Electrochemical Properties of Coenzyme Pyrroloquinolinequinone Using a Di-(4-Pyridyl) Disulfide Modified Gold Electrode under Acidic Conditions. *Bull. Chem. Soc. Jpn.* **1993**, *66* (4), 1289−1291.
(7) Kanninen, P.; Ruiz, V.; Kallio, T.; Anoshkin, I. V.; Kauppinen, E. I.; Kontturi, K. Simple Immobilization of Pyrroloquinoline Quinone on Few-Walled Carbon Nanotubes. *Electrochem. Commun.* **2010**, *12* (9), 1257−1260.
(8) Kay, C. W. M.; Mennenga, B.; Görisch, H.; Bittl, R. Structure of the Pyrroloquinoline Quinone Radical in Quinoprotein Ethanol Dehydrogenase. *J. Biol. Chem.* **2006**, *281* (3), 1470−1476.
(9) Matsumura, H.; Umezawa, K.; Takeda, K.; Sugimoto, N.; Ishida, T.; Samejima, M.; Ohno, H.; Yoshida, M.; Igarashi, K.; Nakamura, N. Discovery of a Eukaryotic Pyrroloquinoline Quinone-Dependent Oxidoreductase Belonging to a New Auxiliary Activity Family in the Database of Carbohydrate-Active Enzymes. *PLoS One* **2014**, *9* (8), No. e104851.
(10) Turbe-Doan, A.; Record, E.; Lombard, V.; Kumar, R.; Levasseur, A.; Henrissat, B.; Garron, M.-L. Trichoderma reesei Dehydrogenase, a Pyrroloquinoline Quinone-Dependent Member of Auxiliary Activity Family 12 of the Carbohydrate-Active Enzymes Database: Functional and Structural Characterization. *Appl. Environ. Microbiol.* **2019**, *85* (24), No. e00964−19.
(11) Jonscher, K. R.; Chowanadisai, W.; Rucker, R. B. Pyrroloquinoline-Quinone Is More Than an Antioxidant: A Vitamin-like Accessory Factor Important in Health and Disease Prevention. *Biomolecules* **2021**, *11* (10), 1441.
(12) Bollella, P.; Katz, E. Enzyme-Based Biosensors: Tackling Electron Transfer Issues. *Sensors* **2020**, *20* (12), 3517.
(13) Oubrie, A. Structure and Mechanism of Soluble Glucose Dehydrogenase and Other PQQ-Dependent Enzymes. *Biochim. Biophys. Acta, Proteins Proteomics* **2003**, *1647*, 143−151.
(14) Takeda, K.; Igarashi, K.; Yoshida, M.; Nakamura, N. Discovery of a Novel Quinohemoprotein from a Eukaryote and Its Application in Electrochemical Devices. *Bioelectrochemistry* **2020**, *131*, 107372.
(15) Takeda, K.; Matsumura, H.; Ishida, T.; Samejima, M.; Ohno, H.; Yoshida, M.; Igarashi, K.; Nakamura, N. Characterization of a Novel PQQ-Dependent Quinohemoprotein Pyranose Dehydrogenase from Classified into Auxiliary Activities Family 12 in Carbohydrate-Active Enzymes. *PLoS One* **2015**, *10* (2), No. e0115722.
(16) Takeda, K.; Umezawa, K.; Várnai, A.; Eijsink, V. G. H.; Igarashi, K.; Yoshida, M.; Nakamura, N. Fungal PQQ-Dependent Dehydrogenases and Their Potential in Biocatalysis. *Curr. Opin. Chem. Biol.* **2019**, *49*, 113−121.
(17) Takeda, K.; Matsumura, H.; Ishida, T.; Yoshida, M.; Igarashi, K.; Samejima, M.; Ohno, H.; Nakamura, N. pH-Dependent Electron Transfer Reaction and Direct Bioelectrocatalysis of the Quinohemoprotein Pyranose Dehydrogenase. *Biochem. Biophys. Res. Commun.* **2016**, *477* (3), 369−373.
(18) Takeda, K.; Minami, T.; Yoshida, M.; Igarashi, K.; Nakamura, N. Direct Bioelectrocatalysis via Interdomain Electron Transfer of Fungal Pyrroloquinoline Quinone-Dependent Pyranose Dehydrogenase Depending on the Alkyl Chain Lengths of Self-assembled Monolayers. *Electrochemistry* **2024**, *92* (2), 022011.
(19) Armstrong, F. A. Recent Developments in Dynamic Electrochemical Studies of Adsorbed Enzymes and Their Active Sites. *Curr. Opin. Chem. Biol.* **2005**, *9* (2), 110−117.
(20) Fourmond, V.; Léger, C. Protein Electrochemistry: Questions and Answers. *Adv. Biochem. Eng. Biotechnol.* **2016**, *158*, 1−41.
(21) Kano, K. Fundamental Insight into Redox Enzyme-Based Bioelectrocatalysis. *Biosci., Biotechnol., Biochem.* **2022**, *86* (2), 141−156.
(22) Kano, K. Fundamentals and Applications of Redox Enzyme-Functionalized Electrode Reactions. *Electrochemistry* **2019**, *87* (6), 301−311.
(23) Bollella, P.; Gorton, L.; Antiochia, R. Direct Electron Transfer of Dehydrogenases for Development of 3rd Generation Biosensors and Enzymatic Fuel Cells. *Sensors* **2018**, *18* (5), 1319.
(24) Chen, H.; Simoska, O.; Lim, K.; Grattieri, M.; Yuan, M. W.; Dong, F. Y.; Lee, Y. S.; Beaver, K.; Weliwatte, S.; Gaffney, E. M.; Minteer, S. D. Fundamentals, Applications, and Future Directions of Bioelectrocatalysis. *Chem. Rev.* **2020**, *120* (23), 12903−12993.
(25) Del Barrio, M.; Sensi, M.; Orain, C.; Baffert, C.; Dementin, S.; Fourmond, V.; Léger, C. Electrochemical Investigations of Hydrogenases and Other Enzymes That Produce and Use Solar Fuels. *Acc. Chem. Res.* **2018**, *51* (3), 769−777.
(26) Adachi, T.; Kaida, Y.; Kitazumi, Y.; Shirai, O.; Kano, K. Bioelectrocatalytic Performance of D-Fructose Dehydrogenase. *Bioelectrochemistry* **2019**, *129*, 1−9.
(27) Schachinger, F.; Chang, H. C.; Scheiblbrandner, S.; Ludwig, R. Amperometric Biosensors Based on Direct Electron Transfer Enzymes. *Molecules* **2021**, *26* (15), 4525.
(28) Takeda, K.; Nakamura, N. Direct Electron Transfer Process of Pyrroloquinoline Quinone-Dependent and Flavin Adenine Dinucleotide-Dependent Dehydrogenases: Fundamentals and Applications. *Curr. Opin. Electrochem.* **2021**, *29*, 100747.
(29) Ikeda, T.; Kobayashi, D.; Matsushita, F.; Sagara, T.; Niki, K. Bioelectrocatalysis at Electrodes Coated with Alcohol Dehydrogenase, a Quinohemoprotein with Heme *c* Serving as a Built-in Mediator. *J. Electroanal. Chem.* **1993**, *361*, 221−228.
(30) Kartashov, A. V.; Serafini, G.; Dong, M. D.; Shipovskov, S.; Gazaryan, I.; Besenbacher, F.; Ferapontova, E. E. Long-Range Electron Transfer in Recombinant Peroxidases Anisotropically Orientated on Gold Electrodes. *Phys. Chem. Chem. Phys.* **2010**, *12* (34), 10098−10107.
(31) Siritanaratkul, B.; Megarity, C. F.; Roberts, T. G.; Samuels, T. O. M.; Winkler, M.; Warner, J. H.; Happe, T.; Armstrong, F. A. Transfer of Photosynthetic $NADP^+$/NADPH Recycling Activity to a Porous Metal Oxide for Highly Specific, Electrochemically-driven Organic Synthesis. *Chem. Sci.* **2017**, *8* (6), 4579−4586.
(32) Takeda, K.; Kusuoka, R.; Birrell, J. A.; Yoshida, M.; Igarashi, K.; Nakamura, N. Bioelectrocatalysis Based on Direct Electron Transfer of Fungal Pyrroloquinoline Quinone-Dependent Dehydrogenase Lacking the Cytochrome Domain. *Electrochim. Acta* **2020**, *359*, 136982.
(33) Takeda, K.; Kusuoka, R.; Inukai, M.; Igarashi, K.; Ohno, H.; Nakamura, N. An Amperometric Biosensor of L-Fucose in Urine for The First Screening Test of Cancer. *Biosens. Bioelectron.* **2021**, *174*, 112831.
(34) Adachi, T.; Fujii, T.; Honda, M.; Kitazumi, Y.; Shirai, O.; Kano, K. Direct Electron Transfer-Type Bioelectrocatalysis of FAD-Dependent Glucose Dehydrogenase Using Porous Gold Electrodes and Enzymatically Implanted Platinum Nanoclusters. *Bioelectrochemistry* **2020**, *133*, 107457.
(35) Zayats, M.; Katz, E.; Baron, R.; Willner, I. Reconstitution of Apo-glucose Dehydrogenase on Pyrroloquinoline Quinone-Functionalized Au Nanoparticles Yields an Electrically Contacted Biocatalyst. *J. Am. Chem. Soc.* **2005**, *127* (35), 12400−12406.
(36) Ivnitski, D.; Atanassov, P.; Apblett, C. Direct Bioelectrocatalysis of PQQ-Dependent Glucose Dehydrogenase. *Electroanal* **2007**, *19* (15), 1562−1568.

https://doi.org/10.1021/acscatal.4c02319
ACS Catal. 2024, 14, 12242−12250

(37) Flexer, V.; Durand, F.; Tsujimura, S.; Mano, N. Efficient Direct Electron Transfer of PQQ-Glucose Dehydrogenase on Carbon Cryogel Electrodes at Neutral pH. *Anal. Chem.* **2011**, *83* (14), 5721−5727.
(38) Murata, K.; Kajiya, K.; Nakamura, N.; Ohno, H. Direct Electrochemistry of Bilirubin Oxidase on Three-Dimensional Gold Nanoparticle Electrodes and Its Application in a Biofuel Cell. *Energy Environ. Sci.* **2009**, *2*, 1280−1285.
(39) Frens, G. Controlled Nucleation for Regulation of Particle-Size in Monodisperse Gold Suspensions. *Nat. Phys. Sci.* **1973**, *241* (105), 20−22.
(40) Galuzzi, B. G.; Mirarchi, A.; Viganò, E. L.; De Gioia, L.; Damiani, C.; Arrigoni, F. Machine Learning for Efficient Prediction of Protein Redox Potential: The Flavoproteins Case. *J. Chem. Inf. Model.* **2022**, *62* (19), 4748−4759.
(41) Kishi, S.; Saito, K.; Kato, Y.; Ishikita, H. Redox Potentials of Ubiquinone, Menaquinone, Phylloquinone, and Plastoquinone in Aqueous Solution. *Photosynth. Res.* **2017**, *134*, 193−200.
(42) Silverstein, P. T.; Rosé, R. J. Dependence of Quinone Electrochemistry on Solvent Polarity and pH. *J. Electrochem. Soc.* **2022**, *169*, 045502.
(43) Fourmond, V. QSoas: A Versatile Software for Data Analysis. *Anal. Chem.* **2016**, *88* (10), 5050−5052.
(44) Hirst, J. Elucidating The Mechanisms of Coupled Electron Transfer and Catalytic Reactions by Protein Film Voltammetry. *Biochim. Biophys. Acta, Bioenerg.* **2006**, *1757* (4), 225−239.
(45) Takeda, K.; Ishida, T.; Yoshida, M.; Samejima, M.; Ohno, H.; Igarashi, K.; Nakamura, N. Crystal Structure of the Catalytic and Cytochrome b Domains in a Eukaryotic Pyrroloquinoline Quinone-Dependent Dehydrogenase. *Appl. Environ. Microbiol.* **2019**, *85* (24), No. e01692−19.
(46) Kim, Y. R.; Kim, R. S.; Kang, S. K.; Choi, M. G.; Kim, H. Y.; Cho, D.; Lee, J. Y.; Chang, S. K.; Chung, T. D. Modulation of Quinone PCET Reaction by Ca^{2+} Ion Captured by Calix[4]quinone in Water. *J. Am. Chem. Soc.* **2013**, *135* (50), 18957−18967.
(47) Laviron, E. General Expression of the Linear Potential Sweep Voltammogram in the Case of Diffusionless Electrochemical Systems. *J. Electroanal. Chem. Interfacial Electrochem.* **1979**, *101* (1), 19−28.

https://doi.org/10.1021/acscatal.4c02319
ACS Catal. 2024, 14, 12242−12250